ISBN: 978-3-95450-234-9 ISSN: 2673-5504 doi:10.18429/JACoW-SRF2023-MOPMB003

FLUX EXPULSION LENS: CONCEPT AND MEASUREMENTS

D. A. Turner[1,*], I. González Díaz-Palacio[2], W. Hillert[2], T. Koettig[1], A. Macpherson[1], G. Rosaz[1], N. Stapley[1], A. Gallifa Terricabras[1], M. Wenskat[2]
[1]CERN, Geneva, Switzerland
[2]Institute of Nanostructures and Solid State Physics, Universität Hamburg, Germany

Abstract

A magnetic flux expulsion lens (MFEL) has been designed and built at CERN. This device uses closed topology conduction cooling of samples to quantify magnetic flux expulsion of superconductors, and allows for systematic measurements of the cooling dynamics and the magnetic response during the superconducting transition. Measurements for bulk Nb, cold worked Nb, sputtered Nb on Cu, and SIS multilayer structures are given. Preliminary results for both sample characterisation of expulsion dynamics, and observation of an enhanced flux expulsion in SIS samples are also reported.

INTRODUCTION

During the transition from the normal conducting (NC) state to the superconducting (SC) state, a perfect SC will expel all ambient magnetic field (B_a) from its volume, i.e. no B field is present within the volume of a SC whilst in the Meissner state. However, for imperfect SC's, impurities and defects within the sample impede flux expulsion, leaving magnetic flux trapped within the SC as vortices. For SRF cavities, the trapped vortices can result in localised heating on the RF surface, which then contributes to the surface resistance (R_s) and reduces the maximum Q_0 of the cavity.

It is well documented that cavity performance is affected by the cooling dynamics, with both the temperature gradient (dT) and the cooling rate as the SC transitions into the Meissner state at T_c [1] correlating with expelled magnetic flux. Within the literature, cool down versus cavity performance improvements have been detailed for slow cooling rates for cavities in a horizontal orientation [2, 3], and fast cooling (high dT) for cavities in a vertical orientation [4–6]. Interpreting flux expulsion efficiency of SRF cavities in terms of flux pinning dynamics is not necessarily straightforward, as an increased spatial thermal gradient (dT/dx) increases the de-pinning force on the flux line, and decreases the probability of a flux line interacting with a pinning site.

In order to establish an assessment of magnetic flux expulsion in materials used for SRF cavities, without the complications of cavity geometry and orientation on flux dynamics during the SC transition, a dedicated flux expulsion measurement system has been developed at CERN. This system, known as the Magnetic Flux Expulsion Lens or MFEL, measures the magnetic flux expulsion of macroscopic samples under controlled thermo-magnetic conditions.

MAGNETIC FLUX EXPULSION LENS

The MFEL, designed and built at CERN, is a simple laboratory device to quantify magnetic flux trapping in samples considered for SRF materials. The MFEL works by applying heat pulses to the sample such that it transitions out of and back to the Meissner state, with the key to the MFEL being the sample geometry, which is a flat annulus geometry (90 mm outer diameter with a 6 mm inner aperture). For this geometry, the outer edge of the sample is in contact with an isothermal cold source, whilst the heat pulse is applied at the inner radius of the annulus. This causes the sample to transition from the SC to the NC state, with the transition propagating radially through the sample. At the end of the heat pulse, the Meissner transition front is driven from the outer radius by the cold source to the centre aperture by the thermal gradient. The extent to which the magnetic flux is driven into the central aperture provides a quantitative measure of the associated flux pinning within the sample. Further, variation of deposited energy from the heat pulse permits measurement of flux expulsion efficiency as a function of thermal gradient, while the time structure of the observed magnetic response offers insight into the thermo-electric dynamics of the transition. The concept of the MFEL flux dynamics is shown in Figs. 1b-1e with the corresponding measurement observables given in Fig. 1a.

Realisation

The MFEL is an axially symmetric device based on an annulus sample that undergoes pulsed heating at the inner radius, while maintaining a thermal connection to a cold source at the outer radius. The magnetic response of the MFEL is measured by a flux gate (Bartington Mag-01H probe) positioned on axis, normal to the sample surface, such that it is sensitive to the flux density traversing the annulus aperture. In addition, thermometry (calibrated CERNOX CX-1050-SD-HT-1.4L with standard Lakeshore acquisition system) is installed at inner and outer edges of the sample and the cold source. Both the magnetic field probe and the temperature (T) sensor are read throughout the heat pulse cycle, with readout rates of 20 Hz and 10 Hz respectively. This readout rate is sufficient for accurate digitising of the thermo-magnetic transition. The heat pulse is provided by a pulsed resistor connected to the sample by a Cu nose cone. A labelled cross section is shown in Fig. 2, which also portrays the heat path through the facility.

For operation, the MFEL is mounted in a vacuum chamber with a Cu base plate that serves as the cooling interface between cold source and MFEL. The vacuum chamber is

* daniel.andrew.turner@cern.ch

ISBN: 978-3-95450-234-9 ISSN: 2673-5504 doi:10.18429/JACoW-SRF2023-MOPMB003

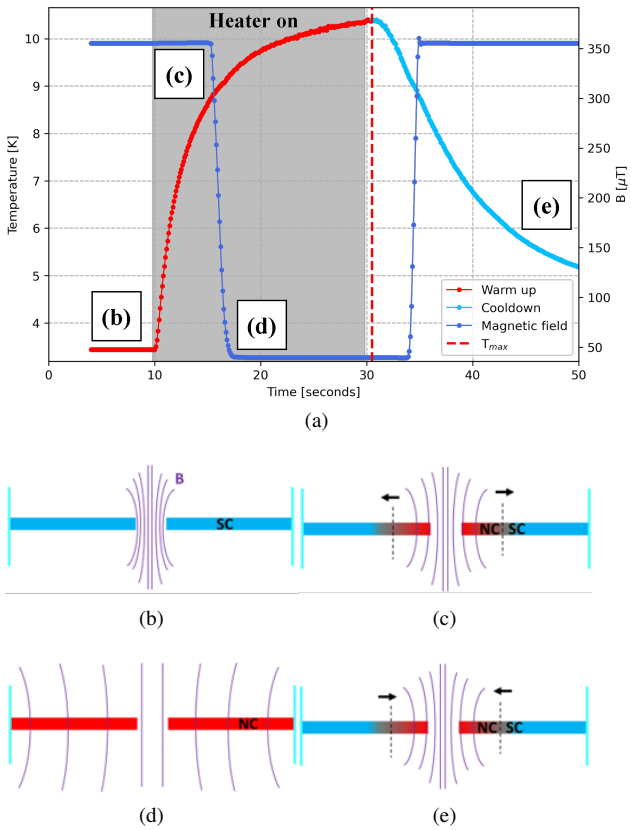

Figure 1: A simple pulse and the corresponding flux dynamics at each stage.

connected to a cold source, such that the MFEL (and sample) is conduction cooled via the interface. This design allows the cold source to be either a standard LHe bath in a conventional cryostat, or a cryocooler installation: both have been used and validated at CERN.

Heat pulses are produced by a pulsing a 50 Ω resistive heater connected via the conductive nose cone to the sample. All contact points for both thermal transfer and T measurement are put under spring loaded compression to ensure minimal thermal contact resistance, and Indium gaskets are used to increase the contact surfaces to the sample.

Operation

With the MFEL inserted into the cryostat, the standard measurement setup adopted at CERN is a simple cool down in a liquid helium (LHe) cryostat, such that the vacuum chamber is fully immersed in the LHe bath with 1 bar vapour pressure. After initial measurements at this cryostat pressure, the cryostat bath T is lowered by regulated pumping of the cryostat vapour pressure. For the MFEL, lower LHe bath T corresponds to an increased achievable thermal gradient across the sample. For a given cryostat pressure, the heat pulse duration is set such that the sample transitions above the critical temperature T_c of the sample material, and that the transition to the NC state extends across the full sample.

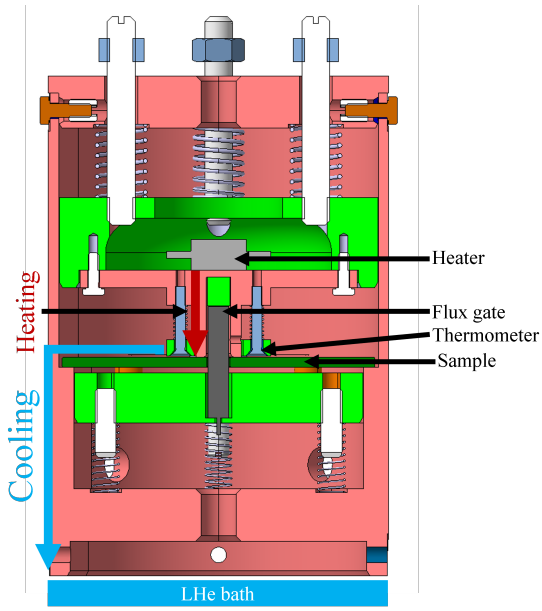

Figure 2: A cross section of the magnetic flux expulsion lens.

The sample is initially in the SC state, and all unpinned magnetic flux has been constrained into the aperture as shown in Fig. 1b. On application of a heat pulse the sample is heated and transitions to the NC state with the flux lines redistributed over the full sample area, with the SC/NC boundary expanding radially outwards over the duration of the heating, as shown in Fig. 1c. This results in a reduced flux density at the probe, and hence a reduced B field reading. With the sample in the NC state the B field is that of B_a, as shown in Fig. 1d. Once the heater is switched off, the sample re-cools from the outside such that the NC/SC boundary moves towards the aperture as shown in Fig. 1e, again constraining the flux lines to the central aperture, producing an increased B field reading. Before repeating this measurement cycle, the system is left to fully thermalise.

Variation of heat pulse duration coupled with measurements taken at different cold bath T constitute the data set taken for each sample, with each data set consisting of over 1000 heat pulse cycles.

Analysis

The transition to/from the SC state is analysed for each heat pulse cycle, in order to assess both the level of magnetic flux expulsion, and the characteristics of the transition dynamics. An example of the analysis is shown in Fig. 3.

Due to limitations in the acquisition readout, it can be seen that the time series T data is an over-sampled measurement, due to an acquisition rate that is half that of the B-field probe. Given that the T data does not rapidly vary on time scales of the B field transition, this oversampling can be corrected by averaging over every second point (as seen by processed T data in Fig. 3).

ISBN: 978-3-95450-234-9 ISSN: 2673-5504 doi:10.18429/JACoW-SRF2023-MOPMB003

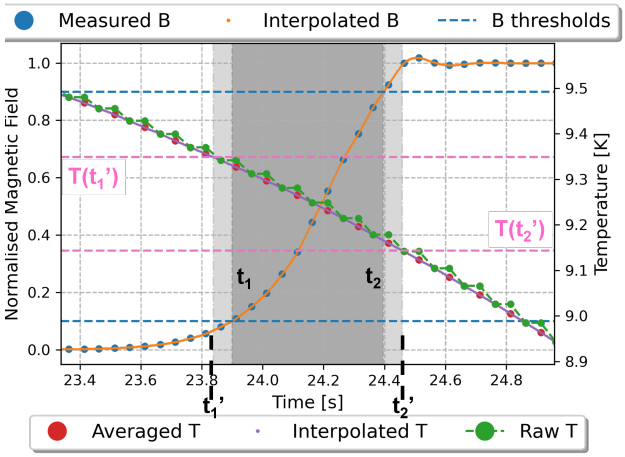

Figure 3: An example transition in the B field and T as the sample transitions into the superconducting state.

In order to compare between different samples, and to systematically evaluate the B field transition duration, the B field data is normalised by taking $B - B_{NC}/B_{SC} - B_{NC}$; this implies that the normalised value is 0 when the sample is NC, and 1 when it is at a stable SC state (taken at the end of the heat pulse cycle). Given that no specific dynamics modelling is prescribed to the transition, both the B field and the T are simply interpolated using a 20-point cubic-spline on each discrete time series data.

To determine a reliable measure of the B field transition duration, thresholds (typically 10-90%) are applied to the the interpolated normalised B field data to determine the start and end times of the transition, (t_1 and t_2 respectively). The associated transition duration is shown in Fig. 3 as the dark grey area. However, in order to remove the influence of the user defined thresholds, the transition duration is corrected by linear extrapolation to a transition time given by $(t_2 - t_1)/(0.9 - 0.1)$. The corrected transition duration and the associated start and end times (t'_1 and t'_2), shown by the light grey area in Fig. 3. This method is used as it minimises the influence of the gradual roll-on/roll-off effects in the B field measurement at the start/end of the transition, and thus improves the time resolution of the transition.

The T's at t'_1 and t'_2 are used to determine the change in transition T, and is defined as $dT = T(t'_1) - T(t'_2))$, which then permits an estimate of the spatial thermal gradient ∇T. Assuming a constant thermal gradient across the sample, ∇T can be approximated as:

$$\nabla T = \frac{dT}{dx} = \frac{dT}{r_{outer} - r_{aperture}} = \frac{dT}{0.042}[\mathrm{K/m}] \quad (1)$$

The flux expulsion of a sample can be evaluated in terms of the effective B field: $B_{eff} = B_{SC}/B_{NC}$ as a function of ∇T.

RESULTS

The MFEL has been used to test a wide variety of SRF related samples, with all recent measurements done at the CERN Cryolab Facility in a standard LHe cryostat. To establish a baseline, bulk Niobium samples were initially considered, and as experience with the MFEL increased, measurements moved to both thin film Nb on Copper and SIS multilayer samples on Nb substrates.

Bulk Nb

Initially, 3 mm thick bulk high RRR Niobium samples have been tested as baseline, as a comparison to other materials. All bulk Niobium samples were taken from the same RRR=300 Niobium sheet as delivered from the supplier with no additional surface treatments performed. From Fig. 4 the baseline bulk Nb had a sharp, linear increase in B_{eff} as a function of ∇T, with a maximum expulsion of 2.4 times that of B_a ($\approx 90\,\mu T$).

Cold Rolled Nb

Taken from the baseline sample set, several samples were cold worked by cross-directional cold rolling to induce mechanical defects. The degree of cold rolling is defined by the reduction in sample thickness, and is representative of the induced plastic strain, giving enhanced crystalline defects in the surface that act as pinning sites within the superconductor. As such, the un-annealed cold-worked samples were expected to exhibit increased flux trapping.

Measurements show that reduction of the bulk niobium sample thickness by 20 or 30% produce a similar B_{eff}(T) with a linear trend that is again linear in ∇T, but is significantly reduced in comparison with the un-worked bulk Niobium sample. Similarly the 50% reduction sample has an even further reduction in B_{eff}, and exhibits almost complete flux trapping independent of ∇T.

This observed substantial decrease in B_{eff}(T) due to cold-working is in line with flux becoming trapped due to the increased number of pinning sites. This will be confirmed by measurement of these samples after high T annealing (≈600 °C - 1000 °C) - at present ongoing.

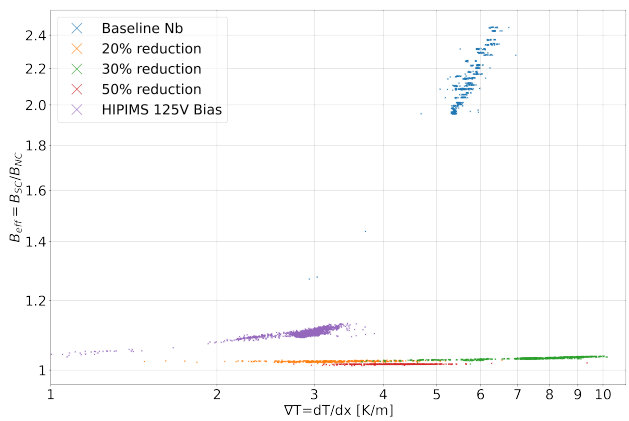

Figure 4: Flux expulsion as a function of ∇T for Nb samples.

ISBN: 978-3-95450-234-9 ISSN: 2673-5504 doi:10.18429/JACoW-SRF2023-MOPMB003

Sputtered Niobium on Copper

For Nb on Cu micron thick films, three samples have been prepared and measured, each with a niobium layer on the order of microns thick. The samples have been prepared by the CERN Vacuum Coatings section using the HIPIMS process [7]. Samples were prepared with different coating process parameters in an effort to optimise the coating process. Initial results show that the Cu substrate can play a non-negligible role in the flux expulsion process, with thermo-electric currents on the Cu contributing to the dynamics.

As can be seen from Fig. 4 the HIPIMS sample response can be compared to the other Nb samples. For the same experimental setup, the HIPIMS sample has a reduced ∇T range due to the thermal path provided by the Cu substrate (due to its higher thermal conductivity); this alternative heat path limits the thermal gradient in the SC layer.

This limitation in maximum ∇T for HIPIMS samples means that the expulsion at 5 K m^{-1} is difficult to measure, making direct comparison with Nb samples more indirect. Still, at $\nabla T \approx 3$ K m^{-1}, the expulsion is $\approx$ 10%, implying that the expulsion is weak, but above the level of the cold worked samples. The degree of expulsion is undergoing further study, as it is suspected that the grain boundaries in the thin film growth contribute to the number pinning sites in the sample, and plays a role in the significant flux trapping observed, despite the limited volume of the SC layer.

SIS Multilayers

Multilayer samples have been prepared at Universität Hamburg by the process of Plasma-enhanced Atomic Layer Deposition (PEALD) [8], and are composed of thin films (smaller than the London penetration depth) of SC and insulator (SIS), with the aim to establish an engineered surface with improved RF performance. In terms of the samples prepared, the substrate is a 2.8 mm thick Nb substrate, with a pre-deposition annealing at 800 °C to remove any stress present within the Nb. The PEALD deposition of the multilayer structure then consists of superconducting 60 nm thin films of NbTiN or NbN, and in some cases have a 15 nm insulating layer of AlN. The samples measured are listed in Table 1.

Table 1: Samples Produced by DESY

Nb - pre-deposition anneal at 800 °C
Nb/NbTiN
Nb/AlN/NbTiN
Nb/AlN/NbN

Based on PEALD qualification measurements, the SIS samples are known to have SC layers with a low T_c relative to what is typically expected from the thin film material, and it is only with a high T post-deposition anneal that the expected T_c performance is recovered. For example, a Nb/NbTiN layer without the post-deposition anneal exhibits a T_c between 7-8 K, which increases up to ≈16 K after a post-deposition anneal [8]. For the results presented in this section, the SIS multilayer samples were measured prior to the post-deposition anneal, and the S-layer T_c was both low and below the T_c of the Nb substrate, such that it was expected that the thin film would not impact the results.

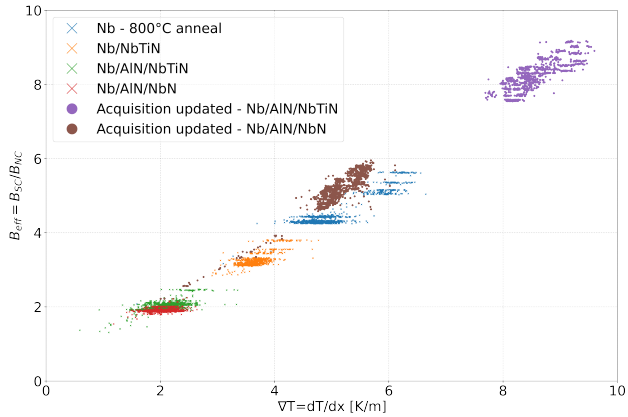

Figure 5: Magnetic flux expulsion as a function of thermal gradient for multilayer samples.

The results of the flux expulsion measurements of the SIS sample prior to their post deposition anneal are given in Fig. 5, and as seen by the clear common linear relationship of B_{eff} as a function of ∇T, the Nb substrate is dominating the flux expulsion behaviour. This is to be expected as the T_c of the thin film is lower than that of the substrate. Still, the consistent linear relationship indicates that B_{eff} does not change between samples, and varies only with ∇T. I.e.- the thin films on the surface are not in the SC regime when the Nb transitions, and as the films are thin with a low T_c, thus no further expulsion is observed at the thin films T_c, as B is not fully expelled from the film. Further, Fig. 5 indicates that there is no influence in B_{eff} due to the presence of the insulating layer, and there is no impact on the ∇T of the MFEL due to the insulating layer.

Interestingly, the B_{eff} is much greater than that for Nb Baseline presented in the previous section. However, this is due to the Nb substrate, as for the SIS samples a different material supplier and preparation of the bulk Nb was used. Specifically, the SIS substrate material was given pre-deposition high T annealing step, which is known to remove a large amount of the pinning sites [9].

Transition Dynamics

Given the variety of samples tested, a direct comparison of the superconducting transition dynamics is best seen not in terms of time series data plots, but as a B field as a function of T. For the samples discussed, Fig. 6 shows such a plot, where the expelled B field is represented by the normalised B field ($B - B_{NC}/B_{SC} - B_{NC}$). There are clear differences in the characteristic curves for the different samples, with the key differences noted as:

- **Bulk Nb:** A clean roll of measure B field with T corresponding to a uniform material sample.

ISBN: 978-3-95450-234-9 ISSN: 2673-5504 doi:10.18429/JACoW-SRF2023-MOPMB003

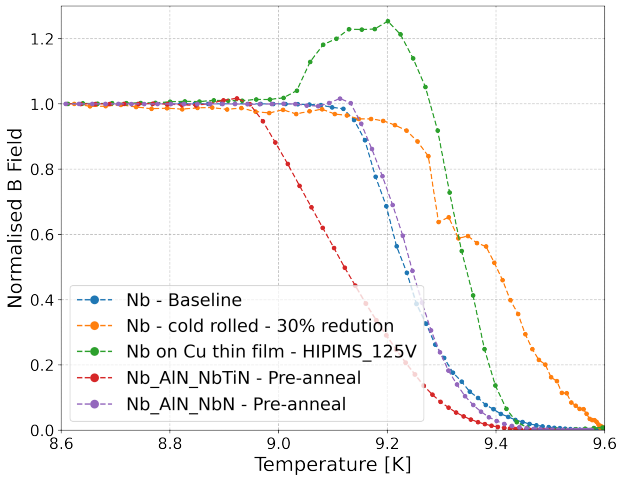

Figure 6: The B field as a function of T as the sample cools from the NC regime to the SC regime.

- **Cold worked Nb:** A distinct two step expulsion pattern consistent with a non-negligible surface damage layer.
- **HiPIMS micron thick Nb on Cu:** clear indications of thermo-electric current generated B field as the sample transitions in/out of the fully SC state.
- **SIS Multilayers:** Small scale B field enhancement as the sample transitions in/out of the fully SC state. This effect is noticeably weaker than the enhancement seen on HiPIMS samples, and given the SIS structure, is suspected to be of screening current origin rather than the thermo-electric current generated.

Flux Pumping

At time of submission, a single SIS multilayer sample had undergone post deposition annealing and was measured in the MFEL. The sample in question was the SIS multilayer with a Nb/AlN/NbTiN structure, and was post deposition annealed at T = 900 °C for 1 h to increase the T_c of the NbTiN layer [8]. On measurement in the MFEL, the sample displayed a S-layer T_c for the NbTiN in excess of 15 K, and as a result, only partial flux reentry into the sample was observed when heated to a T in the $T_{c,Nb}<T<T_{c,NbTiN}$ range.

However, what was not expected was that the expelled flux (as measured by B_{SC} at the end of each measurement cycle) increased with successive heat pulse cycles. The effect is clearly shown in Fig. 7, where each data point corresponds to a separate heat pulse cycle. This incremental change in B_SC with successive thermal pulsing appears to eventually saturate. Further, only upon increasing the heat pulse power such that the maximum T of the sample exceeded $T_{c,NbTiN}$, was the SIS structure fully converted to the normal conducting state, and on re-cooling, the subsequent B_SC reset back to its initial level.

This reproducible observation is consistent with a novel form of flux pumping, where trapped flux is progressively 'ratcheted' out of the superconductor by successive thermal cycles. This 'ratcheting' phenomenon occurs due to the presence of two different superconducting layers with different T_c, suggesting that the high T_c film prevents flux relaxation over repeated transitioning of the Nb substrate. With sufficient iterations, the expulsion that is significantly higher than the pre-annealed level.

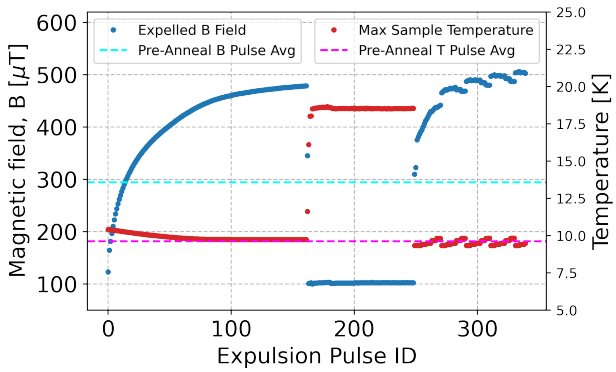

Figure 7: Expelled B field (B_{SC}) verses heat pulse cycle for the post-deposition annealed Nb/AlN/NbTiN sample.

SUMMARY

The magnetic flux expulsion lens has been designed, built, and is fully operating at CERN, and is able to reproducibly measure flux expulsion signatures on bulk Nb, cold worked Nb, micron thick Nb on Cu and SIS multilayer samples. Measurements show the expected correlation between flux expulsion and applied spatial thermal gradient, and that almost any degree of cold working induces significant flux trapping, confirming the necessity for post cold work annealing.

With the measurement of micron thick Nb on Cu, there is clear observational evidence that the substrate plays a significant role, with thermo-electric currents directly contributing to the expulsion dynamics.

Finally, while SIS multilayer measurements for samples without post-deposition annealing have flux expulsion dominated by the substrate, the post-deposition annealed sample exhibits enhanced flux expulsion through controlled heat pulsing. Due to the SIS structure with differing T_c, magnetic flux is recursively ratcheted out of the sample,in a process akin to magnetic flux pumping. Such a mechanism has to potential to significantly reduce trapped flux in SRF cavities, independent of the cavity orientation, and may offer a novel means to improve RF performance.

ACKNOWLEDGEMENTS

Prof. I. Ben-Zvi from BNL for insightful discussions. Prof. V. Mertinger and team at the Institute of Physical Metallurgy Metal forming and Nanotechnology, University of Miskolc, Hungary for the preparation of cold rolled Niobium samples, S. Pfeiffer of the CERN Mechanical and Materials Engineering Group for structural analysis of SIS samples, G. Rosaz, S.Leith, and C. Pereira from the CERN vacuum Coatings section for the preparation of the HiPIMS samples, P. Schneider of the CERN Mechanical Design Office,

ISBN: 978-3-95450-234-9 ISSN: 2673-5504 doi:10.18429/JACoW-SRF2023-MOPMB003

J. Bastard and the team from the CERN Cryogenics Lab for infrastructure and support, L. S. Preece, R. Zierold and Prof. R. H. Blick, and A. Ivanov for development of the initial prototype. The work performed at University of Hamburg is supported by NOVALIS 05K22GUD.

REFERENCES

[1] O. Kugeler *et al.*, "Manipulating the Intrinsic Quality Factor by Thermal Cycling and Magnetic Fields", in *Proc. SRF'09*, Berlin, Germany, Sep. 2009, paper TUPPO053, pp. 352–354.

[2] N. R. A. Valles *et al.*, "Cornell ERL Main Linac 7-cell Cavity Performance in Horizontal Test Cryomodule Qualifications", in *Proc. IPAC'13*, Shanghai, China, May 2013, paper WEPWO068, pp. 2459–2461.

[3] J.-M. Vogt, O. Kugeler, and J. Knobloch, "Impact of cool-down conditions at T_c on the superconducting rf cavity quality factor", *Phys. Rev. Spec. Top. Accel. Beams*, vol. 16, p. 102002, Oct. 2013. doi:10.1103/PhysRevSTAB.16.102002

[4] A. Romanenko *et al.*, "Dependence of the residual surface resistance of superconducting radio frequency cavities on the cooling dynamics around T_c", *J. Appl. Phys.*, vol. 115, p. 184903, 2014. doi:10.1063/1.4875655

[5] A. Romanenko *et al.*, "Ultra-high quality factors in superconducting niobium cavities in ambient magnetic fields up to 190 mG", *Appl. Phys. Lett.*, vol. 105, p. 234103, 2014. doi:10.1063/1.4903808

[6] T. Kubo, "Flux trapping in superconducting accelerating cavities during cooling down with a spatial temperature gradient", *Prog. Theor. Exp. Phys.*, vol. 2016, p. 053G01, 2016. doi:10.1093/ptep/ptw049

[7] G. Rosaz, A. Bartkowska, C. P. Carlos, T. Richard, and M. Taborelli, "Niobium thin film thickness profile tailoring on complex shape substrates using unbalanced biased high power impulse magnetron sputtering", *Surf. Coat. Technol.*, vol. 436, p. 128306, 2022, doi:10.1016/j.surfcoat.2022.128306

[8] I. G. Díaz-Palacio, "Thermal annealing of superconducting niobium titanium nitride thin films deposited by plasmaenhanced atomic layer deposition", submitted for publication.

[9] T. Junginger *et al.*, "Field of first magnetic flux entry and pinning strength of superconductors for rf application measured with muon spin rotation", *Phys. Rev. Accel. Beams*, vol. 21, no. 3, p. 032002, 2018. doi:10.1103/PhysRevAccelBeams.21.032002